Dynamics of Excess Free Volume in Semicrystalline PEEK Studied by Positron Annihilation

H. Nakanishi† and Y. C. Jean*

Department of Chemistry, University of Missouri—Kansas City, Kansas City, Missouri 64110

Received January 22, 1991; Revised Manuscript Received July 8, 1991

ABSTRACT: The dynamical behavior of the free-volume creation and its relaxation in the amorphous regions of two-phase PEEK were monitored during isothermal crystallization as a function of annealing time up to 60 min at 160 °C (T_g = 145 °C) by positron annihilation lifetime measurements. The kinetics of the isothermal crystallization was analyzed by the Avrami equation. The development of the relative crystallinity, mean free-volume hole size, and relative free-volume fraction as a function of annealing time were obtained from the observed o-Ps lifetime and intensity using analytical equations derived from a quantum mechanical model. The maximum values of the mean free-volume hole size and the fraction as a function of annealing were observed and were explained in terms of two competing processes, i.e., the creation of the excess free volume at the boundary of the growing crystal spherulite and the relaxation of the excess free volume diffusing into the amorphous region.

Introduction

The dynamical behavior of free volume in polymer systems has been a central interest for many years since it is directly related with many viscoelastic properties of polymers. Among the many experimental techniques available to study the free-volume behavior, the positron annihilation lifetime (PAL) method has a unique advantage over others as demonstrated in various polymer systems[1] since PAL gives direct information on the microscopic free volume.

In a previous study[2] we showed that the positronium (Ps) formation probability in semicrystalline polymer PEEK, poly(aryl ether ether ketone) or poly(oxy-1,4-phenyleneoxy-1,4-phenylenecarbonyl-1,4-phenylene), is proportional to the degree of the crystallinity and that Ps forms at free-volume sites in the amorphous regions of two-phase PEEK. In the present study, we will demonstrate another unique feature of the PAL technique by monitoring the dynamical behavior of the free-volume creation during isothermal crystallization of PEEK at temperatures above the glass transition temperature, T_g.

Experimental Section

Amorphous PEEK films with thickness 0.25 mm were purchased from ICI (Imperial Chemicals, Inc.) Americas. Each of the 2 × 4 cm² amorphous films was placed between two aluminum plates with identical size to prevent the film from curling and to improve thermal contact. The annealing was performed by immersing the wrapped sample into a constant-temperature silicone oil bath where the temperature was maintained at 160 ± 0.5 °C, which is 15 °C above the glass transition temperature of amorphous PEEK (T_g = 145 °C).[3] After each annealing with time listed in Table I, each sample was quenched immediately at 0 °C by immersing the sample into an ice–water bath. This quenching procedure preserves the free-volume properties nearly constant[4] during the PAL measurements which take approximately 30 min for 1 million counts at room temperature.

Each annealed sample sheet was cut into eight 1 × 1 cm² square pieces. A 25-μCi ^{22}NaCl aqueous solution (2.5 μL) sealed between 6-μm-thick (1.6 mg/cm²) aluminum foil was placed at the center of a 1 × 1 cm² piece of PEEK film prepared by the annealing procedure described above. Additional layers of film were then added, resulting in a sample having four identical pieces (total thickness 1.02 mm) of the PEEK sheets on each side of the positron source. More than 99% of the positrons were estimated to stop and annihilate inside the PEEK samples by using a source correction program.[5] The PAL measurements were performed using a conventional fast-timing apparatus. The time resolution for the spectrometer was determined by collecting a PAL spectrum from degassed pure water. Two Gaussian resolution functions were found (fwhm's = 260 and 345 ps at 80 and 20%, respectively) in the water spectrum using the program RESOLUTION.[6] The source correction due to the positron annihilation in the aluminum source holder was estimated to be 10.3% by using an equation reported previously[5] with a measured average lifetime of 176 ps in aluminum foil.

Three lifetime components were resolved from each PAL spectrum containing a million counts by the computer program PATFIT.[6] Three-component analysis yields consistently better stability and χ^2 parameters than two- and four-component analyses (two-component results give a large χ^2 (>2) and four-component results give standard deviations larger than fitted values). The first two lifetime components with lifetimes τ_1 = 130 ± 10 ps and τ_2 = 460 ± 10 ps and intensities I_1 = 30 ± 4% and I_2 = 50 ± 4% were assigned to p-Ps self-annihilation and free-positron annihilation in the sample. The third component with lifetime $\tau_3 \approx 1.8$ ns and intensity $I_3 \approx 20\%$ was attributed to the o-Ps annihilating in the free-volume sites[2] such the small thickness of the crystalline lamellae (presumably on the order of 2 nm)[7] should allow all o-Ps to diffuse to free-volume sites.

Table I
PAL Data and Calculated PEEK Crystallinity (X_c), Free Volume Size (V_f), and Fractional Free Volume (F_r) as a Function of Annealing Time (t) at 160 °C

t, min	τ_3, ps	I_3, %	X_c, %	V_f, nm³	F_r
0.0	1811 ± 13	22.5 ± 0.3	3.3 ± 1.5	0.080 ± 0.001	1.00 ± 0.01
1.0	1835 ± 18	22.1 ± 0.4	5.3 ± 2.0	0.082 ± 0.001	1.01 ± 0.01
1.5	1836 ± 18	21.9 ± 0.4	6.2 ± 2.0	0.082 ± 0.001	1.00 ± 0.01
2.0	1857 ± 18	21.9 ± 0.4	6.5 ± 2.0	0.084 ± 0.001	1.02 ± 0.01
2.5	1851 ± 19	21.6 ± 0.4	8.0 ± 2.0	0.083 ± 0.001	1.00 ± 0.01
3.5	1861 ± 20	20.1 ± 0.4	15.3 ± 2.0	0.084 ± 0.001	0.94 ± 0.01
5.0	1849 ± 28	19.7 ± 0.4	17.6 ± 2.0	0.083 ± 0.001	0.91 ± 0.01
5.5	1839 ± 21	19.4 ± 0.4	19.0 ± 2.0	0.082 ± 0.001	0.89 ± 0.01
6.0	1840 ± 20	19.4 ± 0.4	19.3 ± 2.0	0.082 ± 0.001	0.89 ± 0.01
8.0	1823 ± 21	19.0 ± 0.4	21.1 ± 2.0	0.081 ± 0.001	0.85 ± 0.01
9.0	1815 ± 21	18.9 ± 0.4	21.8 ± 2.0	0.080 ± 0.001	0.84 ± 0.01
12.0	1814 ± 21	19.3 ± 0.4	19.6 ± 2.0	0.080 ± 0.001	0.85 ± 0.01
15.0	1803 ± 17	19.0 ± 0.3	21.3 ± 1.5	0.079 ± 0.001	0.83 ± 0.01
17.5	1814 ± 19	19.0 ± 0.3	21.2 ± 1.5	0.080 ± 0.001	0.84 ± 0.01
20.0	1801 ± 8	19.1 ± 0.2	20.5 ± 1.0	0.079 ± 0.001	0.84 ± 0.01
25.0	1790 ± 23	19.0 ± 0.3	21.1 ± 1.5	0.078 ± 0.001	0.82 ± 0.01
30.0	1785 ± 10	18.8 ± 0.3	22.3 ± 1.5	0.077 ± 0.001	0.81 ± 0.01
60.0	1795 ± 16	18.9 ± 0.3	21.7 ± 1.5	0.078 ± 0.001	0.82 ± 0.01

† Present address: Department of Medicinal Chemistry and Pharmacognosy, University of Illinois at Chicago, Chicago, IL 60680.

0024-9297/91/2224-6618$02.50/0 © 1991 American Chemical Society

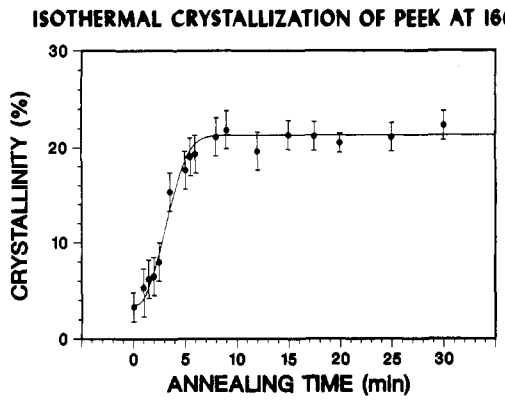

Figure 1. Annealing time dependence of the percent crystallinity calculated from eq 1 using o-Ps intensities listed in Table I. The solid line is calculated by the Avrami equation (2) with fitted parameters. (The line > 6 min was not fitted and was drawn at zero slope for guiding the eye.)

The lifetime and the intensity of this component were found to be very sensitive to the free-volume size and the degree of the crystallinity in the PEEK sample, respectively.[2]

Results and Discussion

The results of the PAL data analysis for the PEEK samples with annealing time 0–60 min at 160 °C immediately followed by quenching at 0 °C are listed in Table I. In a previous study[2] on the PEEK polymer, we found that the Ps formation probability or I_3 is linearly related to the percent crystallinity X_c as

$$X_c = -(5.1 \pm 0.2)I_3 + (118 \pm 10) \quad (1)$$

The calculated values for the percent crystallinity from eq 1 are listed in Table I, and the annealing time dependence is shown in Figure 1. The maximum crystallization rate observed by the PAL technique is near 3 min. The logarithm of the maximum crystallization time (t_c) is a parabolic function of the isothermal annealing temperature (T_c). In PEEK, Blundell and Osborn found that $t_c \sim 0.1$ min at $T_c \sim 225$ °C.[7] The crystallization rate is very sensitive to the T_c. For example, the time to reach maximum rate varies from 11.4 to 2.8 min as the T_c changes from 160 to 164 °C.[4] The sigmoidal crystallization curve at early time as shown in Figure 1 is very similar to the curve observed by the DSC measurements[4] at T_c = 164 °C. A small discrepancy in the T_c may be due to the different sample preparation methods used and/or the different initial crystallinity.

The kinetics of the isothermal crystallization can be analyzed by the Avrami equation[4] in which the development of the relative crystallinity $X_r(t) = [X_c(t) - X_c(0)]/[X_c(\infty) - X_c(0)]$ is given by

$$-\ln [1 - X_r(t)] = Zt^n \quad (2)$$

where Z and n are the parameters depending on the crystallization mechanism. Using $X_c(\infty) = 21.3$ and $X_c(0) = 3.5$, the log of the left side of eq 2 is plotted against the log of the annealing time t in Figure 2 up to t = 6 min, since the data rapidly deviate from the Avrami curve after the initial crystallization. The Avrami parameters n and Z were determined from the slope and the y intercept at log (t) = 0 using least-squares analysis as $n = 2.3 \pm 0.1$ and log $Z = -5.3 \pm 0.3$. Our results are similar to those (n = 2.6 and log $Z = -5$) observed by DSC measurements for amorphous PEEK at T_c = 160 °C.[4] The percent crystallinity calculated from the Avrami equation with fitted parameters was shown in Figure 1 with a solid line,

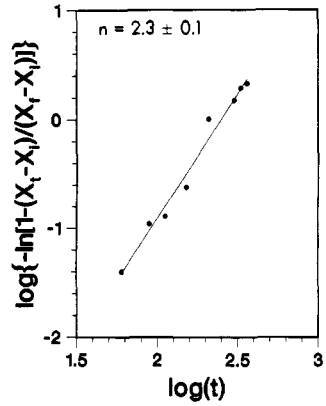

Figure 2. Avrami equation analysis of the isothermal crystallization of PEEK at 160 °C. The parameters Z and n were determined by the least-squares fit as n = 2.3 and Z = −5.3.

indicating that the Avrami equation represents the isothermal crystallization of PEEK quite well.

The parameters n and Z provide a diagnostic insight for the crystallization mechanism. For example, a spherical growth of crystal with sporadic nucleation leads to n = 4 and $Z = (2/3)\pi g^3 l$, where g is the radial growth rate and l is the rate of the nucleation sites. If the nuclei are predetermined, n = 3 and $Z = (4/3)\pi g^3 L$ can be obtained, where L is the number of predetermined nucleation sites. If rates of crystallization are diffusion controlled, which occurs in the presence of high concentrations of noncrystallizable impurities, the value of n becomes half of the corresponding values of n due to the $r = gt^{1/2}$ dependence, where r is the radius of a crystal.[8] Our value of 2.3 and the DSC value of 2.6 suggest that the crystallization mechanism is predetermined or that there is simultaneous nucleation of the spherulites. The n value, lower than 3, however, indicates that the diffusion process may have a small contribution since the noncrystallizable amorphous PEEK may act as impurities.

By assuming a simple quantum mechanical model where a Ps resides in an infinite spherical potential of radius R_0 with an electron layer of thickness ΔR, the following analytical relation between o-Ps lifetime τ_3 and the free-volume radius R ($=R_0 - \Delta R$) has been obtained:[2,9,10,11]

$$\tau_3^{-1} = 2\{1 - R/R_0 + (1/2\pi) \sin (2\pi R/R_0)\} \text{ (ns}^{-1}\text{)} \quad (3)$$

The value of ΔR was found to be 1.66 Å by fitting eq 3 to observed o-Ps lifetimes in molecular crystals with known vacancy sizes.[12] The average size of the free-volume sites in the amorphous regions of PEEK was then estimated from the o-Ps lifetimes listed in Table I and plotted in Figure 3. The average free-volume size observed reaches a maximum 84 Å^3 at ~3.5 min of the annealing time at 160 °C and exponentially decreases to 78 Å^3.

This effect can be explained by the difference in the time constants for the crystallization and the relaxation of the amorphous region. Since the density of the crystals of PEEK (1.378 or 1.400 g/cm^3)[3,7] is higher than that of the amorphous PEEK (1.264 g/cm^3)[3], the rapid crystallization creates voids at the interface between the crystal spherulites and the amorphous region. This leads to the increase of the average free-volume size at the beginning of the isothermal annealing. As the crystallization slows down after ~4 min (see Figure 1), the stress at the surface is annealed away and the relaxation process becomes more dominant, so that the decrease in the average free-volume size is expected.

We employed a simple model to elaborate this effect. The relaxation of the free volume can be expressed as[13]

$$\frac{dV_f}{dt} = \frac{-[V_f - V_f(\infty)]}{t(V_f,T)} + R_x \quad (4)$$

The first term in eq 4 was previously proposed by Kovacs, where V_f is the momentary free volume, $V_f(\infty)$ is the equilibrium free volume at temperature T, and $t(V_f,T)$ is the momentary value of the relaxation time which is dependent on both V_f and T. The second term was added to account for the production rate of the free volume due to the crystallization, which may be approximated by the rate of the crystallization, i.e., $R_x = C\,dX_c(t)/dt$, where C is a constant. An explicit expression the free-volume dependence of the relaxation time or the diffusion constant is given by the well-known Doolittle equation.[14] Here we found that a constant value gives a reasonable approximation. In general cases, this may seem too crude an approximation, since the relaxation time usually changes many orders of magnitude. In our case, however, (1) the distribution of the excess free volume is presumed to be localized at the interface, (2) the amorphous region is large compared to the crystalline region (79–96.5%), and (3) the free-volume fraction does not change very much in the amorphous region; thus diffusion of the excess free volume may be well approximated by the constant value.

The rate of the crystallization, dX_c/dt, is given by the Avrami equation with the values Z and n obtained previously. Constants C and t are the only adjustable parameters in the differential equation (4). We solved this equation by using IMSL subroutines for differential equations and adjusted values of C and t so that the fit between the experimental and the calculated values of V_f became optimum. The best values we obtained were C = 1.9 and t = 5 min. The calculated values of V_f from eq 4 are plotted in Figure 3 as a solid line.

The agreement is good, in spite of the crude approximation used. The observed V_f continuously decreases after the annealing time of 20 min, whereas the calculated V_f reaches an asymptotic value. This discrepancy may be due to the constant relaxation time used, since the relaxation time becomes larger and larger as the free-volume fraction reaches the equilibrium value according to the Doolittle equation. On the other hand, if the Doolittle equation is valid, the initial relaxation time should be much smaller and thus the calculated V_f should exhibit a quite pronounced dip before reaching the maximum. As seen in Figure 3, there is no dip observed. Therefore, we conclude that the Doolittle type free-volume relaxation does not apply to our system while the crystallization is dominant, and it only applies after the crystallization slows down.

In the previous PAL study on the temperature dependence of τ_3 and I_3 in an amine-cured epoxy polymer,[15] we found that the fractional free volume F_v (%) can be expressed from the o-Ps lifetime parameters as

$$F_v = CV_fI_3 \quad (5)$$

where V_f (Å^3) is the average volume of free-volume holes, assuming spherical geometry. The coefficient C was determined for the epoxy polymer to be 2.5 by comparing the thermal expansion coefficient obtained using eq 5 with that measured by thermal expansion.[16] For the case of amorphous or slightly crystalline PEEK, the thermal expansion coefficient cannot be determined because of the tendency of PEEK to spontaneously crystallize once the sample is heated above T_g. Therefore, we calculated a relative free-volume fraction, $F_r(t) = V_f(t)\,I_3(t)/V_f(0)\,I_3(0)$, and plotted Figure 4. The solid line shown was generated from the calculated V_f value times a smoothed

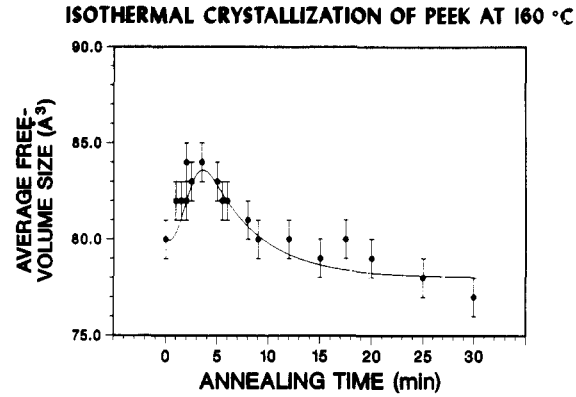

Figure 3. Annealing time dependence of the average free-volume hole size calculated from eq 3 using o-Ps lifetimes. The solid line is a solution of differential equation (4) based on the approximation discussed in the text.

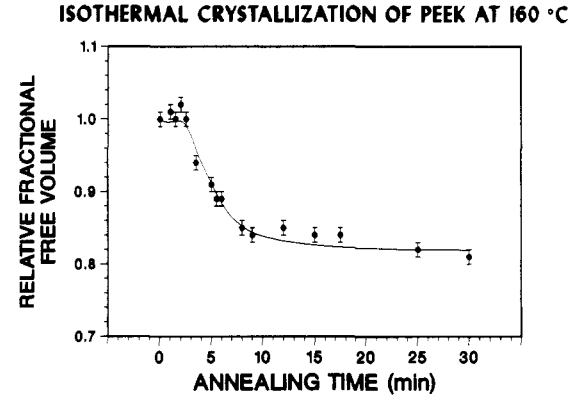

Figure 4. Annealing time dependence of the relative free-volume fraction calculated from eq 5. The solid line is a normalized product of the smoothed o-Ps intensities and the solution of eq 4.

value of I_3 with a normalization constant $^1/_{18}$. At the initial stage of the isothermal annealing up to 2.5 min, the creation and the relaxation of the free volume are almost counterbalanced so that the observed free-volume fraction remains almost constant. A total of 20% free volume was annealed away. This agrees well with the fact that approximately 20% of the amorphous regions are crystallized during the annealing at 160 °C so that 20% reduction in the free-volume fraction should be observed since there is no free volume in the crystal, assuming that the fractions of the free volume in the amorphous region at the initial and the final states are the same. This also confirms the conclusion of the previous PEEK study that the Ps formation probability is proportional to the degrees of crystallinity and that Ps forms at free-volume sites in the amorphous regions.[2]

Conclusion

The dynamical behavior of the free-volume creation and its relaxation in the amorphous regions of two-phase PEEK were monitored during isothermal crystallization at 160 °C up to 60 min by positron annihilation lifetime measurements. The crystallinity of the PEEK during the annealing process was obtained from the positronium formation intensities. The kinetics of the isothermal crystallization was analyzed by the Avrami equation, and the parameters Z and n were determined by least-squares analysis as $\log Z = -5.3 \pm 0.3$ and $n = 2.3 \pm 0.1$. The values are in very good agreement with values from DSC measurements.[4]

The average size of the free-volume holes was obtained from the o-Ps lifetime using an analytical equation derived

from a simple quantum mechanical model.[2,9] The observed maximum of free-volume hole sizes was explained by two competing processes, i.e., the creation of the excess free volume at the boundary of the growing crystal spherulite due to the difference in the densities and the relaxation of the excess free volume diffusing into the amorphous region. A simple diffusion model was employed with an added perturbation term to account for the creation rate of the free volume given by the first time derivative of the Avrami equation. In spite of the crude approximation used for the relaxation time constant, a good agreement was observed between the measured and the calculated V_f's. It is concluded that the Doolittle type free-volume relaxation does not apply to our system with localized excess free volume while the crystallization is dominant, and it only applies after the production of the excess free volume slows down.

The positron annihilation lifetime method used for the analysis of the excess free-volume relaxation may be generalized to study the relaxation of the free volume by temperature and pressure jumps and by mechanical deformations.

Acknowledgment. This research has been supported by the McDonnell Douglas Independent Research and Development Program and the National Science Foundation (Grant DMR-90040803). Fruitful discussions with Dr. T. C. Sandreczki are acknowledged.

References and Notes

(1) Jean, Y. C. *Microchem. J.* **1990**, *42*, 72.
(2) Nakanishi, H.; Jean, Y. C.; Smith, E. G.; Sandreczki, T. C. *J. Polym. Sci. B* **1989**, *27*, 1419.
(3) Hay, J. N.; Kemmish, D. J.; Langford, J. I.; Rae, A. I. M. *Polym. Commun.* **1984**, *25*, 175.
(4) Cebe, P.; Hong, S. D. *Polymer* **1986**, *27*, 1183.
(5) Schrader, D. C.; Chiu, S. W.; Nakanishi, H.; Rochanakij, S. In *Positron Annihilation*; Jain, P. C., Singru, R. M., Gopinathan, K. P., Eds.; World Scientific: Singapore, 1985; p 822.
(6) Kirkegaard, P.; Eldrup, M.; Mogensen, O. E.; Pedersen, N. J. *Comput. Phys. Commun.* **1981**, *23*, 307.
(7) Blundell, D. J.; Osborn, B. N. *Polymer* **1983**, *24*, 953.
(8) Keith, H. D.; Padden, F. J., Jr. *J. Appl. Phys.* **1964**, *35*, 1286.
(9) Nakanishi, H.; Jean, Y. C. In *Positron and Positronium Chemistry*; Schrader, D. M., Jean, Y. C., Eds.; Elsevier: Amsterdam, The Netherlands, 1988; p 159.
(10) Tao, S. J. *J. Chem. Phys.* **1972**, *56*, 5499.
(11) Eldrup, M.; Lightbody, D.; Sherwood, J. N. *Chem. Phys.* **1981**, *63*, 51.
(12) Nakanishi, H.; Wang, S. J.; Jean, Y. C. In *Positron Annihilation Studies of Fluids*; Sharma, S. C., Eds.; World Scientific: Singapore, 1988; p 292.
(13) Tant, M. R.; Wilkes, G. L. *Polym. Eng. Sci.* **1981**, *21*, 874.
(14) Doolittle, A. K. *J. Appl. Phys.* **1951**, *22*, 1471.
(15) Nakanishi, H.; Wang, Y. Y.; Jean, Y. C.; Sandrecski, T. C. In *Positron Annihilation Studies of Fluids*; Sharma, S. C., Ed.; World Scientific: Singapore, 1988; p 285.
(16) Wang, Y. Y.; Nakanishi, H.; Jean, Y. C. *J. Polym. Sci. B* **1990**, *28*, 1431.

Registry No. PEEK, 31694-16-3.